sustainability

MDPI

Article

Network Reconfiguration Framework for CO_2 Emission Reduction and Line Loss Minimization in Distribution Networks Using Swarm Optimization Algorithms

Wei-Chen Lin [1], Chao-Hsien Hsiao [1], Wei-Tzer Huang [1,*], Kai-Chao Yao [1], Yih-Der Lee [2], Jheng-Lun Jian [2] and Yuan Hsieh [1]

[1] Department of Industrial Education and Technology, National Changhua University of Education, Bao-Shan Campus, No. 2, Shi-Da Road, Changhua 500, Taiwan; wc83@cc.ncue.edu.tw (W.-C.L.); d1231019@mail.ncue.edu.tw (C.-H.H.); kcyao@cc.ncue.edu.tw (K.-C.Y.); yuanhsieh@gmail.com (Y.H.)
[2] National Atomic Research Institute, Taoyuan 325, Taiwan; ydlee@nari.gov.tw (Y.-D.L.); jhenglun@nari.gov.tw (J.-L.J.)
* Correspondence: vichuang@cc.ncue.edu.tw; Tel.: +886-939-828-628

Abstract: This paper presents the development of a generic active distribution network (ADN) operation simulation framework that incorporates selected swarm optimization algorithms (SOAs) for the purpose of reducing CO_2 emissions and line loss minimization through network reconfiguration (NR). The framework has been implemented in the ADN of Taipower. Network data, provided by the Distribution Mapping Management System and Distribution Dispatch Control Center (DDCC) of Taipower, were converted into an OpenDSS script to create ADN models. The SOA is integrated into the framework and utilized to determine the statuses of both four-way and two-way switches in the planning and operating stages, in accordance with the proposed multi-objective function and operational constraints. The weightings for these decisions can be customized by distribution operators to meet their specific requirements. In this paper, the weighting for line loss reduction is set to one for minimizing CO_2 emissions. The numerical results demonstrate that the proposed ADN framework can recommend a feeder switching scheme to distribution operators, aiming to balance feeder loading and minimize the neutral line current. Finally, this approach leads to reduced line losses and minimizes CO_2 emissions. In contrast to relying solely on historical operational experience, this generic ADN reconfiguration framework offers a systematic approach that can significantly contribute to reducing CO_2 emissions and enhancing the operational efficiency of ADNs.

Keywords: CO_2 emissions; line loss; active distribution network; network reconfiguration; swarm optimization algorithms; OpenDSS

Citation: Lin, W.-C.; Hsiao, C.-H.; Huang, W.-T.; Yao, K.-C.; Lee, Y.-D.; Jian, J.-L.; Hsieh, Y. Network Reconfiguration Framework for CO_2 Emission Reduction and Line Loss Minimization in Distribution Networks Using Swarm Optimization Algorithms. *Sustainability* **2024**, *16*, 1493. https://doi.org/10.3390/su16041493

Academic Editor: Ripon Kumar Chakrabortty

Received: 5 December 2023
Revised: 22 January 2024
Accepted: 7 February 2024
Published: 9 February 2024

1. Introduction

The majority of ADNs feature a radial topology, consisting of distribution generations (DGs) and loads arranged to serve both high and low voltage customers. This radial arrangement is chosen for the considerations of its reliability and cost benefits. However, it is acknowledged that the power flow in each branch and bus voltage profile distribution, as well as service reliability, is inferior in radial ADNs compared to that in closed-loop, mesh, and interconnected networks [1].

To address the inherent limitations of radial ADNs, network reconfiguration (NR) has been widely employed in distribution system operations. This involves changing the open and closed statuses of the sectionalizing and tie switches of the feeders [2–8]. Regardless of topology changes, the distribution networks (DNs) must be maintained in a radial type.

In the past decade, advancements in information and communication technology, coupled with the application of artificial intelligence algorithms, have enabled the

realization of smart operations in DNs. Notably, in NR, the solution speed and efficiency have seen significant improvements in large-scale systems, utilizing machine learning, deep learning, and reinforcement learning algorithms [9–12], as well as metaheuristic algorithms [13–19].

Various approaches have been explored, such as the use of the social beetle swarm optimization algorithm [20], two-stage binary swarm optimization [21], selective firefly algorithms [22], the water cycle algorithm [23], hybrid metaheuristic and heuristic algorithms [24], the harmony search algorithm [25], and the fuzzy C-means clustering algorithm [26], among others. These approaches aim to optimize network configurations and switching operations, considering factors like power loss, load balance, and voltage deviation.

Despite the demonstrated capabilities of these algorithms, their practical implementation in large-scale ADNs faces challenges related to acquiring and managing extensive data, including long-term load data, photovoltaic (PV) and wind turbine (WT) generation data, and switch status data. This paper addresses these challenges by incorporating big data into NR problem-solving using swarm optimization algorithms. The goal was to achieve feeder loading balance, ultimately reducing line losses and decreasing CO_2 emissions.

In addition, addressing the challenge of NR in ADNs is particularly complex due to the intermittent power outputs of DGs and the diverse nature of loads in practical ADNs. Therefore, this study was dedicated to developing a platform that leverages SOAs to achieve CO_2 emission reduction and line loss minimization within ADNs. This platform is designed to be efficient and user-friendly, providing distribution operators with a valuable tool to determine optimal feeder switching strategies in order to balance feeder loading, ultimately reducing line losses and CO_2 emissions. The effectiveness of this platform was evaluated through its implementation in Taipower ADNs. This paper is organized into five sections. Section 1 introduces the background and objectives of the study. Section 2 outlines the approach used to model Taipower ADNs. Section 3 elaborates on the integration of NR with swarm optimization algorithms. Section 4 demonstrates the functions of the developed platform and presents the results of numerical simulations. Finally, in Section 5, we provide the conclusion of this research.

2. Modeling of the ADNs

In order to develop a simulation framework within a real ADN, it is crucial to accurately model the distribution feeder. OpenDSS (Version 9.6.1.2), an electric power distribution system simulator, plays a vital role in supporting the integration of DGs and modernizing the grid. This versatile, customizable, and user-friendly tool is increasingly being employed in various research projects [27]. The DN models within OpenDSS encompass most components of a DN, including DGs like PV and WT ones, and the engine can efficiently solve time-series three-phase unbalanced power flow simulations. Moreover, OpenDSS allows the creation of simulation scripts using text files, which simplifies the modeling of extensive DNs, such as those managed by Taipower ADNs. Therefore, OpenDSS was chosen as the simulation engine for the proposed framework. Data regarding DN elements and network topology were extracted from the Distribution Mapping Management System (DMMS) and the Supervisory Control and Data Acquisition (SCADA) system of the DDCC and were then converted into OpenDSS scripts to construct the ADN model. Subsequent sections will detail how to acquire and process the extensive data associated with Taipower ADNs.

2.1. SCADA System in DDCC

The power system comprises three main components: generation, transmission, and distribution systems, which form the vertical structure of the system. The DDCC and the Feeder Dispatch Control Center (FDCC) are situated at the terminus of the Hierarchical Dispatch and Control System (HDCS) within the power system. As a result, network topology data, customer load data, and DG data can be acquired from both the DDCC and

FDCC. The NR problem involves the manipulation of feeder switches within the zones of ADNs, falling under the jurisdiction of a specific DDCC and FDCC. In this research, specific regions within Taipower's ADNs were employed as the sample system. The chosen area encompassed 23 substations, comprising 9 distribution substations (D/Ss), 13 secondary substations (S/Ss), and 1 primary substation (P/S). Each substation accommodated one–three main transformers, with each main transformer connected to five–six feeders. In summary, this specific area comprised a total of 348 feeders.

Figure 1 depicts a section of the SCADA screen within the substation of this particular district. Vital details, such as current and power flows from the feeder, were distinctly displayed on the screen, accessible through the database. Typically, each feeder in Taipower is equipped with two–four feeder terminal units (FTUs) to facilitate feeder automation within ADNs. The FTU measures the manner of power flow and transmits it directly to the FDCC and DDCC using IEC 61850 [28] or DNP 3.0 protocols without any further manipulations. The single line diagrams and photos of the four- and two-way FTUs are also presented in Figure 1a,b. Left- and right-way switches generally constitute the FTUs, and the other two switches of the four-way FTU are for the laterals or high voltage customers. Currently, the underlying standard functions of FTUs are measurement, control, and fault detection [29]. Consequently, the big data of the measured three-phase real and reactive powers is stored in the database in the DDCC, and these data are used for solving emergency, real-time, and short-term operating problems, such as fault detection, isolation, restoration (FDIR), and planned maintenance. In this research, the measured data were used to represent the net load pattern, which was composed of the original loads and DGs of each feeder segment for solving the power flow to obtain the optimal NR. The load modeling method is described in the next subsection.

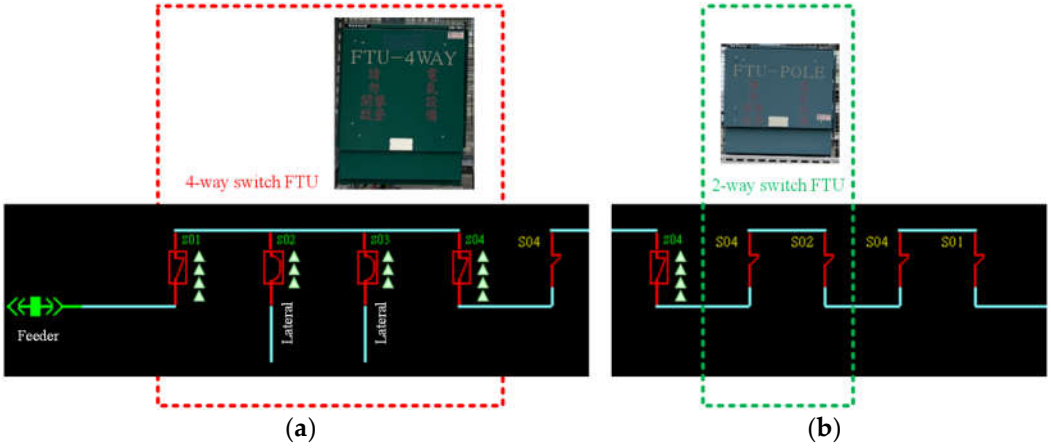

Figure 1. Automatic switches with FTU in a feeder segment in Taipower SCADA system. (**a**) Four-way switch. (**b**) Two-way switch.

2.2. Network Topology Modeling

As illustrated in Figure 2, the model of the ADNs was constructed by converting the following files: "substation (.set)", "switch and transformer (.set)", and "FTU data (.sql)". These files were obtained from the DMMS and SCADA systems of Taipower's DDCC and were transformed into OpenDSS scripts (.dss). The conversion process was implemented using Python programming language, which allowed for the transformation of the three files into their corresponding parts in OpenDSS. These parts encompassed substation, line, line code, load, load shape, DGs, switch, and location scripts, all of which were essential for modeling the ADN. In particular, the load and DG patterns contained within the (.sql) file were converted into (.csv) files. This conversion enabled OpenDSS to execute time-series (hourly) power flow simulations. The OpenDSS scripts were organized into three main sections, namely the substation, branch, and load and DG models, each of which is detailed in the following sections.

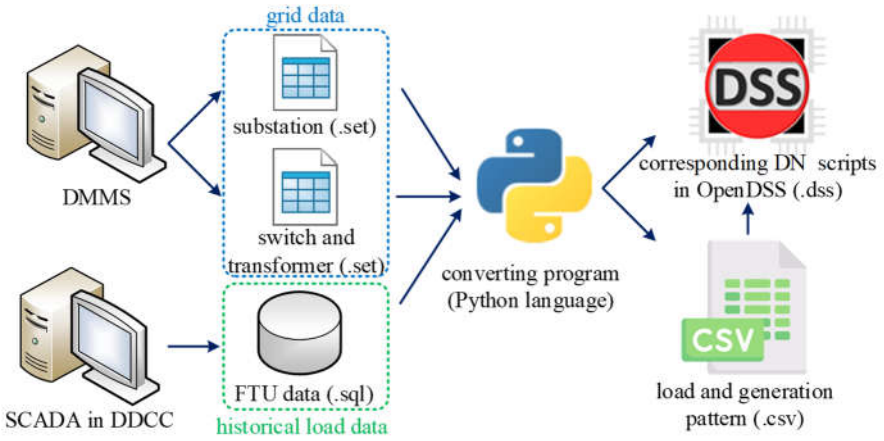

Figure 2. The schematic diagram of data converting processing.

2.2.1. Substation Model

The existing names or codes of substations, main transformers, and feeders were stored in the individual fields of the substation (.set) file. As a result, these interrelated data were employed to establish the link between substations and feeders via the main transformer. Vital parameters, such as the number of windings, short-circuit impedance of the main transformer, base voltage, and per unit values, were included within the substation script to accompany this correlation.

2.2.2. Branch Model

The switch and transformer (.set) files contained a data table with 13 fields representing the relationships between feeders, switches, distribution transformers, and the types and capacities of DGs. These fields are outlined as follows:

- Switch coordinates;
- Latitude and longitude of switch coordinates;
- Switch coordinates of the upstream switch;
- Feeder code to which the switch belongs;
- Switch status;
- Whether the switch is normally opened or not;
- Switch type and code;
- Switch coordinates of the downstream switch (in case of a normally opened switch);
- Feeder code to which the downstream switch belongs (in case of a normally opened switch);
- Pole number or address;
- Conductor type and length;
- DG type and installed capacity.

This dataset could be transformed into a branch model by using line code scripts within OpenDSS. The model included three-phase impedance per unit length based on Taipower's distribution line specifications, such as 500 MCM, 400 MCM, and others. With the connection relationships, latitude and longitude details, line lengths, and line impedance, the line model could be constructed. Furthermore, the geographic information of the area grid could be visualized using Python programming language in conjunction with a graphing library.

2.2.3. Load and DG Models

To analyze the long-term steady-state power flow solution, the critical factor is the load and DG data, owing to their time-varying characteristics. This is particularly significant in ADNs with high DG penetration, as the bidirectional power flow cannot be adequately represented by single-time-point data. Consequently, acquiring a large dataset of customer load and generation data from PV systems and small WTs connected to the ADN is essential to address this challenge. However, obtaining such load and DG data presents practical challenges. In the case of load data, the Advanced Metering Infrastructure (AMI) is not widely implemented in Taipower's ADNs, and privacy concerns limit access to data from some high-voltage customers. As for DG data, information on DGs with an installed capacity of less than 100 kW is not transmitted back to the DDCC in Taipower. Consequently, the metered point returns to the upstream FTU to comprehensively and accurately collect this information.

The FTU's measured data included three-phase active and reactive powers, line currents, and bus voltages within its measurement section, as depicted in Figure 3. Typically, FTUs are installed at the front end and middle section of a feeder. To estimate the loads at each tapped-off point on a feeder, the metered hourly net loads from the measurement sections of the FTUs are divided into the respective loads of high-voltage customers, distribution transformers, laterals, and DGs based on their capacities. Assuming that the hourly measured real and reactive powers are represented as P_{FTU}^{h} and Q_{FTU}^{h}, and there are n tapped-off points in this section, with $C_{DT,i}$ denoting the installed capacity of each distribution transformer, the real and reactive powers of each distribution transformer can be determined by (1).

$$S_{DT,i}^{h} = P_{DT,i}^{h} + jQ_{DT,i}^{h} = (P_{FTU}^{h} + jQ_{FTU}^{h}) \times \frac{C_{DT,i}}{\sum_{i}^{n} C_{DT,i}} \quad (1)$$

Based on the hourly load data obtained at each bus in the feeder, the proposed algorithm allowed for the real-time or periodic optimization of the NR in the ADNs at monthly, seasonal, and annual intervals. This enabled the system to continuously adapt and find optimal solutions to enhance its performance and efficiency.

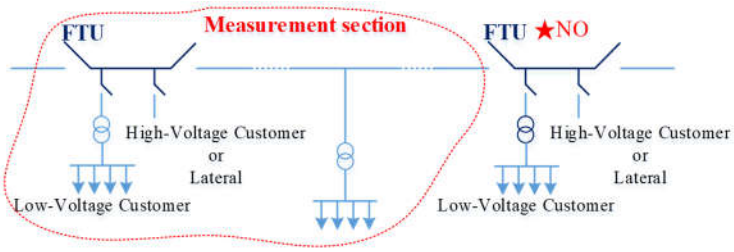

Figure 3. The sketch of the FTU measurement section (the red star represents the normally open point).

3. NR Optimization Algorithm

NR is a complicated problem with strict constraints, and the circuit topology must be kept radial for the coordination of protection relay and to comply with the grid code. In this section, the proposed NR algorithms and their integration with the SOA is discussed.

3.1. NR Algorithms

In general, the topology of ADNs is primarily radial or open-loop. Closed-loop or interconnected networks are typically implemented in areas that require high reliability. Within an open-loop system, after fault detection and isolation, the un-faulted feeder segment can be transferred to other feeders using mechanisms such as normally open tied

switches, sectionalizers, reclosers, ring main units (RMUs), and feeder sectionalizing units (FSUs) to restore the electricity. This strategic approach aims to minimize interruptions and reduce outage durations. The NR problem is to find out the optimal feeder radial topology by operating the normally opened (NO) and normally closed (NC) feeder switches to uniformly distribute feeder segment current and then balance the feeder loading, reduce the line loss, etc. Therefore, the NR algorithm must comply with the radial topology. However, due to the algorithmic randomness, there will not only usually be closed-loop topology but also the islanding branches if the switch status is decided by the agent state of the algorithm. Many studies about NR have been conducted and have proposed approaches to address this challenge. Sekhavatmanesh et al. [30] used the constraints in an algorithm to filter the closed-loop or islanding topology; this method will work well in a simple ADN but will not obtain a feasible solution if the ADN is very large, such as that for the Taipower real system. Prasad et al. [28] identified all feasible radial topologies in advance and stored them in a dataset. The algorithm then selected data from the dataset to ensure the right solution. However, this approach becomes time-consuming for large networks due to the effort involved in obtaining all feasible topologies. In this research, an NR algorithm was proposed and developed. If the NO switches were closed, then the network would have a loop, and the algorithm would determine the switch in this loop according to the topology level. The swarm algorithm would decide to open one of the switches in the loop to restore the radial topology. Through the above process, one set of an NO and NC switch operation was completed, and the topology was changed. The algorithm iterated through this process until all NO switch operations were completed. The flow chart depicting this process is shown in Figure 4.

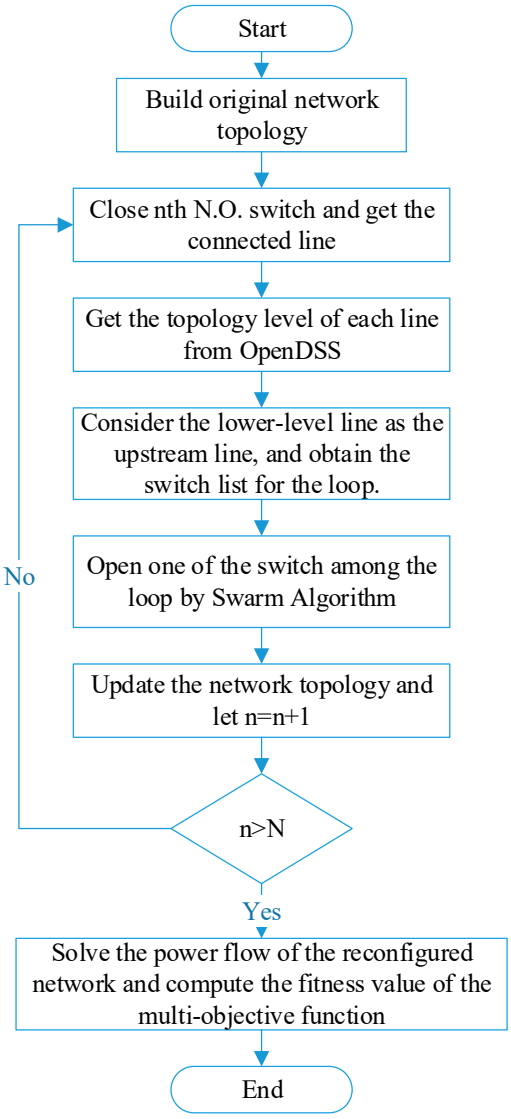

Figure 4. The sketch of FTU measurement section.

Tracking the loop was a challenging technical task in this method because one line may connect to many others, and determining which line formed the loop was unknown from the perspective of a specific line. Fortunately, the network level could be obtained in OpenDSS, allowing for the determination of upstream and downstream relations, as indicated by the numbers in Figure 5. This illustrative diagram depicted two substations and four feeders. The substation was considered level 0, the line connected to it was level 1, and so on. Consequently, scanning the line from the NO switch to the line with the minimum topology level enabled the determination of the loop, as highlighted by different colors in Figure 5. One of the switches in this loop was selected by swarm intelligence, and the circuit topology changed accordingly. This process was sequentially conducted for each NO switch. A new topology was obtained, and the power flow of the new circuit was solved by OpenDSS. The performance of this topology was evaluated by the swarm algorithm based on the power flow results, such as line loss and voltage profile. Figure 5 also illustrates various types of loops generated by closing the NO switches, described as follows:

- The loop within one feeder;
- The loop between two feeders fed by the same transformer;
- The loop between two feeders fed by different transformers in the same substation;
- The loop between two feeders fed by different transformers in different substations.

In general, the 11.4 kV feeders can be transferred to each other by the NO tie switch, regardless of whether they are fed by S/S or D/S; similarly, the 22.8 kV feeders also can be transferred to each other, whether they are fed by D/S or P/S.

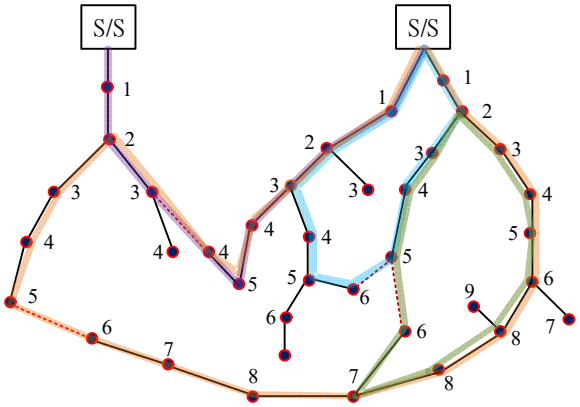

Figure 5. Illustration of topology level and loop (The colors represent different feeders, and the numbers are the bus codes in the original radial feeders).

3.2. Swarm Intelligence Algorithms

Swarm intelligence refers to the collective behavior of a decentralized and self-organized system inspired by biology, nature, and human interactions. This algorithm employs simple mathematics formulated based on the mechanisms observed in swarm systems, such as mimicking the behavior of foraging and natural phenomena, to search for the best solution in each iteration. Unlike methods that rely on derivatives in gradient descent or ascent, swarm intelligence formulations are typically straightforward and require minimal computation time. Consequently, good solutions can be quickly obtained. These types of algorithms are well-suited for addressing optimization problems, such as NR in ADNs. In this research, swarm algorithms were adopted as optimal approaches for selecting the switches to open in the loop described in Figure 5, as illustrated in Figure 6. Each agent of the swarm represented a set of open switches in the loops. The swarm underwent different positions to conduct global and local searches, ultimately finding the best or optimal solution at the end of the iteration. A generic SOA can be expressed as follows:

Step 1. Initialization: initialize a swarm of individuals, such as particles, agents, or solutions, within the search space.
Step 2. Evaluation: evaluate the fitness or objective function value of each individual in the swarm.
Step 3. Iteration or Generation: repeat the update position, evaluation fitness, update personal best, update global best, and termination check steps until a termination criterion is met, for instance, a maximum number of iterations or a satisfactory solution is found.
Step 4. Termination: once the termination criterion is met, the algorithm returns with the best solution found.

In this study, forty-two popular or novel swarm algorithms were investigated and implemented using Python language to determine their effectiveness in solving the NR problem, and the detailed theory and equations can be found in SOA reference [31]. The benchmark function used for evaluation was the Rastrigin function, represented as (2), where A = 10, $(x_i,\ldots,x_N)\in\mathbb{R}^N$, N is the dimension, the global minimum is 0 when $x=(0,0,\ldots,0)$, and the search domain is $-5.12\le x_i\le 5.12$. The ADNs of the Taipower system were very large, so the solving time of the power flow would be very long. Consequently, the algorithm must quickly converge and obtain a feasible solution. Table 1 lists the performance of the 42 algorithms selected in this research. The dimension of the test function was set to 100 to simulate the NR problem, and the correct solution needed to be determined using 100 agents in 100 iterations. The results showed that only the GWO,

EOA, WOA, COA, NMRA, HHO, MRFO, BES, SSA, HGS, VCS, and SMA could obtain the correct solution. However, the VCS and SMA spent too much time in the process.

$$f(x) = AN + \sum_{i=1}^{N-1}\left[x_i^2 - A\cos(2\pi x_i)\right] \quad (2)$$

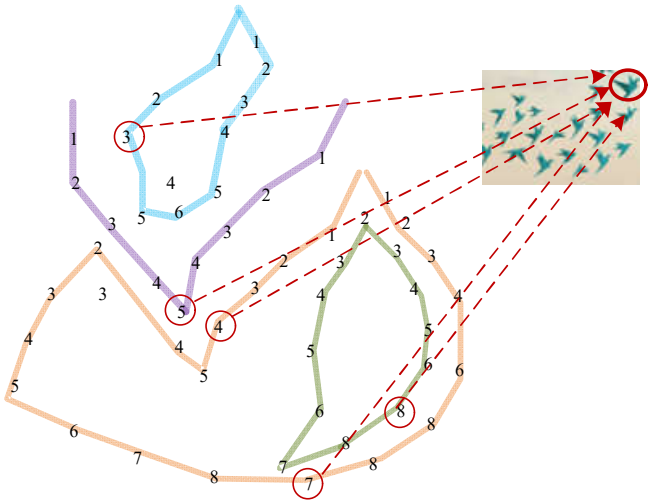

Figure 6. Illustration of a set of open switches in the loops of an agent of the swarm (The colors represent different loops, and the numbers are the bus codes in original radial feeders).

Table 1. Performance of swarm algorithms.

Algorithm	Solution	Runtime(s)
Particle Swarm Optimization (PSO)	1242.19	1.613637
Bacterial Foraging Optimization (BFO)	1463.61	107.155
Cat Swarm Optimization (CSO)	1355.29	14.05538
Artificial Bee Colony (ABC)	491.55	1.712844
Ant Colony Optimization (ACO)	1618.03	14.6655
Cuckoo Search Algorithm (CSA)	1461.39	1.853617
Firefly Algorithm (FFA)	1587.87	49.15207
Fireworks Algorithm (FA)	1294.55	3.847575
Bat Algorithm (BA)	1558.86	1.38656
Fruit-Fly Optimization Algorithm (FOA)	2040.24	7.049848
Gray Wolf Optimizer (GWO)	0.00	1.539688
Social Spider Algorithm (SSOA)	1504.65	0.690324
Ant Lion Optimizer (ALO)	402.63	46.97378
Elephant Herding Optimization (EOA)	0.00	3.564406
Moth Flame Optimization (MFO)	1603.64	7.295122
Elephant Herding Optimization (EHO)	131.34	1.497053
Jaya Algorithm (JA)	1600.77	1.282912
Whale Optimization Algorithm (WOA)	0.00	1.508786
Dragonfly Optimization (DO)	666.44	11.00129
Bird Swarm Algorithm (BSA)	591.46	1.773952
Spotted Hyena Optimizer (SHO)	1499.59	9.781862
Salp Swarm Optimization (SSO)	391.27	1.594091
Swarm Robotics Search and Rescue (SRSR)	83.00	4.74453
Grasshopper Optimization Algorithm (GOA)	790.76	23.5384
Coyote Optimization Algorithm (COA)	0.00	2.418113
Moth Search Algorithm (MSA)	586.16	1.869665
Sea Lion Optimization (SLO)	682.77	1.510401
Wildebeest Herd Optimization (WHO)	740.62	13.97535
Naked Mole-Rat Algorithm (NMRA)	0.00	1.836967

Pathfinder Algorithm (PFA)	15.49	22.0776
Sailfish Optimizer (SFO)	0.15	2.998278
Harris Hawks Optimization (HHO)	0.00	2.901618
Manta Ray Foraging Optimization (MRFO)	0.00	3.15128
Bald Eagle Search (BES)	0.00	4.810156
Sparrow Search Algorithm (SSA)	0.00	3.538787
Hunger Games Search (HGS)	0.00	1.867956
Aquila Optimizer (AO)	0.28	2.288997
Invasive Weed Optimization (IWO)	567.42	6.452828
Biogeography-Based Optimization (BBO)	178.79	15.18734
Virus Colony Search (VCS)	0.00	29.25268
Satin Bowerbird Optimizer (SBO)	336.17	14.31655
Slime Mold Algorithm (SMA)	0.00	35.22056

4. The Developed Framework and Numerical Results

The ADN could be modeled using OpenDSS, and the net load data could be obtained from the DDCC database through the conversion process illustrated in Figure 2. The selected SOAs were integrated to solve the NR of ADNs. This section emphasizes the development of the Generic Active Distribution Network Reconfiguration Framework (GADNRF) using Python language and discusses the numerical results. The GADNRF served as a user-friendly interface (UI) designed for ADN operators.

4.1. Framework Structure and Multi-Objective Function

Figure 7 illustrates the UI of the proposed platform for the GADNRF, and its functions are explained as follows:

- Users can choose whether to operate switches for laterals or exclusively within the main feeder.
- Two simulation modes are available: "fast" and "complete". The "fast" mode utilizes daily average load data for the power flow solution, while the "complete" mode uses complete data.
- Users can choose the weights of the proposed objective function, which are further described below.
- The platform offers a choice of forty-two swarm algorithms, with adjustable parameters for the agent population and iteration count.
- Users can set the year, month, and period of historical load data as the simulation period.
- Multiple target substations can be selected, and the UI displays the main transformers and upstream feeder.
- Geographic information is visually presented for intuitive use.
- Information related to simulation settings is displayed in the text area.
- After the simulation is complete, results and suggestions regarding switch operations are exported to a designated folder.
- Simulation results, including total line loss, line current, neutral current at the feeder front, and geographic information, are depicted as bar charts upon completion of the simulation.

The planning of the aforementioned functions needed to consider reducing CO_2 emissions. Therefore, this research integrated power losses, neutral current reduction, feeder current uniform distribution, mitigation of bus voltage fluctuation, and minimizing switch operation times to establish a multi-objective function.

The five indicators mentioned above can be formulated as individual objective functions in (3)–(7). The formulas f_1~f_5 represent the normalized values corresponding to power loss, neutral current, feeder segment current, bus voltage magnitude, and switch operation times.

$$f_1 = \sum_{i=1}^{n} \frac{P_{i,loss}^{max} - P_{i,loss}}{P_{i,loss}^{max} - P_{i,loss}^{min}} \tag{3}$$

$$f_2 = \frac{I_{i,neutral}^{max} - I_{i,neutral}}{I_{i,neutral}^{max} - I_{i,neutral}^{min}} \tag{4}$$

$$f_3 = \sum_{i=1}^{n} \frac{I_{i,\mathrm{var}}^{max} - I_{i,\mathrm{var}}}{I_{i,\mathrm{var}}^{max} - I_{i,\mathrm{var}}^{min}} \tag{5}$$

$$f_4 = \sum_{i=1}^{n} \frac{V_{i,\mathrm{var}}^{max} - V_{i,\mathrm{var}}}{V_{i,\mathrm{var}}^{max} - V_{i,\mathrm{var}}^{min}} \tag{6}$$

$$f_5 = \sum_{i=1}^{n} \frac{N_{i,switch}^{max} - N_{i,switch}}{N_{i,switch}^{max} - N_{i,switch}^{min}} \tag{7}$$

where $P_{i,loss}$ is the total line loss of *ith* feeder, $I_{i,neutral}$ is the neutral current of the *ith* feeder front, and I_i is the *ith* feeder segment current. Moreover, I_μ is the trimean of them as shown in (8); Q_1, Q_2, and Q_3 are the quartile of them; and I^{var} is the variance of them as shown in (9). Additionally, $V_{i,\mathrm{var}}$ is the average bus voltage magnitude variation of the *ith* feeder and can be calculated by (10), where V_j^{DER} is the *jth* bus voltage magnitude with DG, and V_j is the *jth* bus voltage magnitude without DGs. Finally, $N_{i,switch}$ is the switch operation times of the *ith* feeder.

$$I_\mu = \frac{Q_1 + 2Q_2 + Q_3}{4} \tag{8}$$

$$I^{\mathrm{var}} = \sum_{i}^{n} (I_i - I_\mu)^2 \Big/ n \tag{9}$$

$$V^{\mathrm{var}} = \sum_{j=1}^{m} (V_j^{DER} - V_j)/V_j \Big/ m \tag{10}$$

After normalization and weighting, the multi-objective function is formulated as (11):

$$f = w_1 f_1 + w_2 f_2 + w_3 f_3 + w_4 f_4 + w_5 f_5 \tag{11}$$

which is subject to

$$w_1 + w_2 + w_3 + w_4 + w_5 = 1 \tag{12}$$

$$0.95 \text{ p.u.} \le V_i^{bus} \le 1.03 \text{ p.u.} \quad i = 1, \ldots, n \tag{13}$$

$$I_j^{line} \le 300 \text{ A} \quad j = 1, \ldots, m \tag{14}$$

In (13) and (14), V_i^{bus} is the voltage magnitude of the *ith* bus, *n* is the number of buses, and I_j^{line} is the current magnitude of the *jth* line segment, where 0.95 and 1.03 p.u. represent the values of the under-voltage and over-voltage limits, and 300 A means the maximum ampere capacity under the normal operation of Taipower. Among the above equations, w_i denotes a weighting factor that can adjust for the operating requirement.

The electrical energy in current power systems is generated by a combination of traditional thermal power plants and renewable energy power plants, resulting in the production of gray energy. Consequently, if the line losses can be minimized, there is a corresponding reduction in CO_2 emissions. While the reduction may not be substantial, it does contribute to lowering CO_2 emissions. Therefore, CO_2 emission can be computed by (15) after the convergence of the multi-objective function in (11), where C_{coef} is the CO_2 emission coefficient, NF is the number of feeders, and NSeg is the number of feeder segments.

$$Emission_{CO2} = \sum_{j=1}^{NF} \sum_{k=1}^{NSeg} C_{coef} \cdot P_{jk,loss} \quad (15)$$

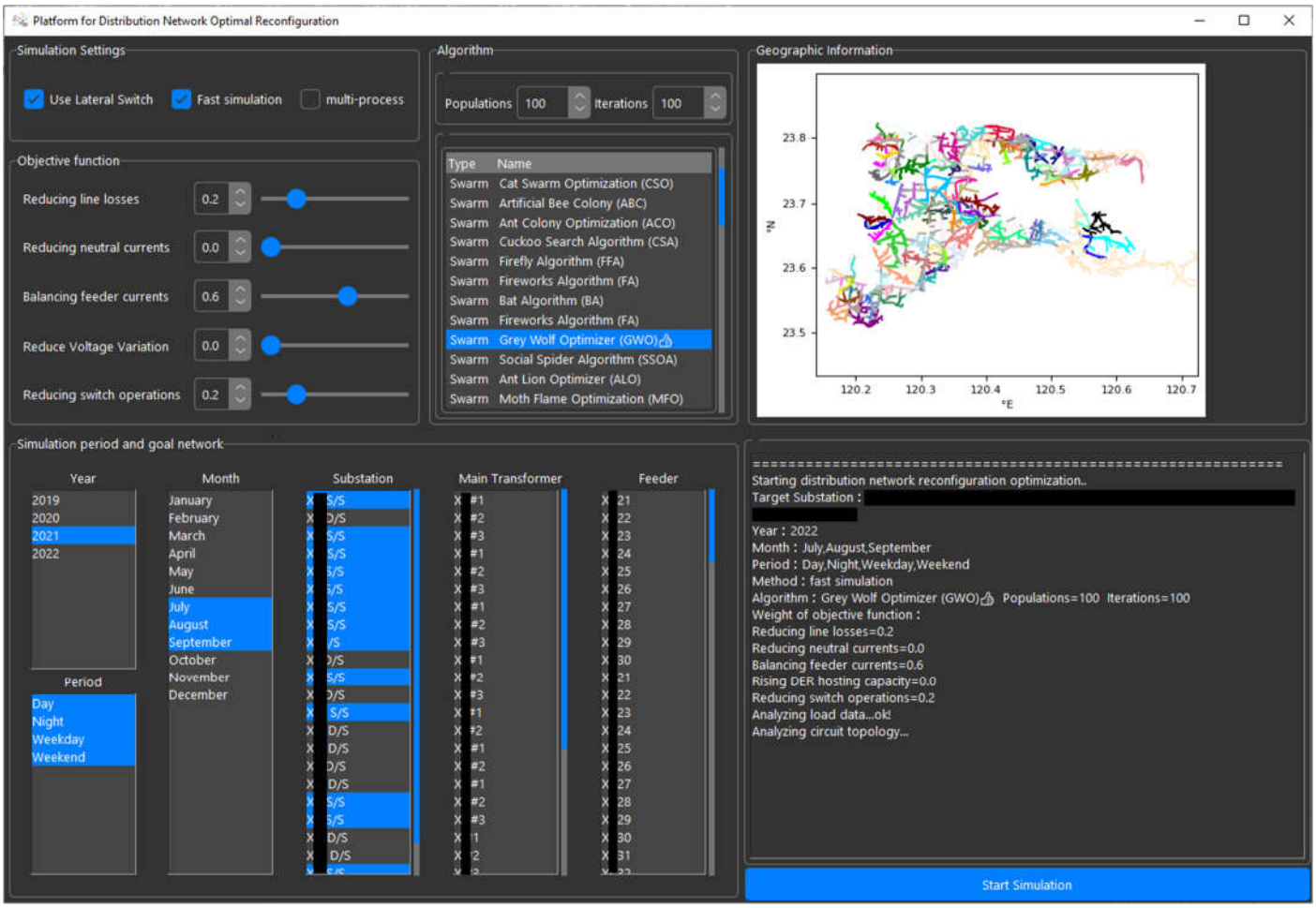

Figure 7. The developed UI of the GADNRF.

4.2. Numerical Results and Discussions

Due to limitations in paper length, this study only simulated and analyzed two cases. The target substation in the proposed platform could be one or more. In this subsection, the numerical results of a single X* S/S and multiple substations are presented as examples. Due to privacy issues with Taipower, the substation and feeder names were masked for confidentiality.

In this study, two cases were simulated, one for an individual substation and another for multiple substations. In the individual substation's case, Figure 8 shows the geographic information of X* S/S. The historical load data in July 2022 was utilized in this simulation. The weight w_1 for the objective function f_1 was set to one for the major consideration of reducing total CO_2 emissions, as line loss was directly proportional to the square

of the magnitude of the feeder current. Once the current was distributed more uniformly in each feeder segment, the minimum total line loss became achievable.

The GWO was selected as the swarm algorithm in this simulation, and the convergence history is shown in Figure 9. Before and after the NR, the simulation results of the maximum line currents of phases A, B, and C, maximum neutral currents, and total line losses of each feeder in X* S/S are depicted in Figures 10–12. The three red bars represent the three-phase current before NR, while the blue bars represent the three-phase current after NR. The results indicated that the maximum current between feeders was more evenly distributed compared to that of the original system. The maximum current in feeder X*32 significantly decreased to 228 A, while for feeder X*28, it increased to 195 A, representing the highest maximum current among all feeders. Furthermore, the maximum currents for all feeders remained within the operational limit of 300 A.

Additionally, the total line loss for feeder X*32 was reduced to 1420 kWh from 1669 kWh during the 12 h simulation. Due to the CO_2 emission coefficient of Taipower being 0.495 kg/kWh, the calculation results for total CO_2 emissions were reduced to 702.9 kg from 826.16 kg. The reduction percentage was 14.92%. Although the objective function weight for the neutral current was set to 0 in this simulation, it still complied with Taipower's limitation of 70 A. The suggested switch operation results are listed in Table 2.

Moreover, the simulation results of multiple substations are presented as follows. Figure 13 shows the geographic information of 3 S/Ss. The WOA was selected to be the algorithm in this simulation. The histogram of the individual phase current at the feeder front of the 3 S/Ss is shown in Figure 14. The probability of high currents at the feeder front was lower after NR, where the frequency of the maximum current over 250 A in this case was reduced from 15 to 9, and the overall maximum current distribution was centralized under 150 A; this helped to reduce CO_2 emissions.

In addition, the simulation results for multiple substations are presented as follows. Figure 14 shows the geographic information of 3 S/Ss, and the WOA was selected as the algorithm in this simulation. The histogram of the individual phase current at the feeder front of the 3 S/Ss is shown in Figure 15. The probability of high currents at the feeder front was lower after NR, where the frequency of the maximum current over 250 A in this case was reduced from 15 to 9, and the overall maximum current distribution was centralized under 150 A. This result also contributed to the reduction of line loss and CO_2 emissions, as illustrated in Figures 16 and 17, respectively. Although the reduction may appear small, it represents an improvement for a specific 12 h period in a localized area. If this NR strategy were applied to the entire national distribution grid, considering annual losses, the benefits would be quite substantial.

Table 2. Switch Operation Suggestion.

Feeder Name	Switch Name	Status (NO/NC)	Feeder Name	Switch Name	Status (NO/NC)
X*23	K01***E60-S01	NC	X*25, X*35	K01***E09-S01	NO
X*25	K02***B56-F01	NC	X*32, X*28	K08***C72-S01	NO
X*25	K04***A62-S01	NC	X*32, X*28	K08***B03-S01	NO
X*28	K08***B32-S01	NC	X*34, X*28	K07***C42-S01	NO
X*30	K03***A11-F01	NC	X*25, X*30	K03***D23-F01	NO
X*30	K04***E08-S01	NC	X*33, X*27	K03***D44-S08	NO
X*32	K08***B18-S01	NC	X*34, X*28	K07***E84-S01	NO
X*32	K10***B50-S01	NC	X*25, X*34	K04***C22-S01	NO
X*33	K03***D44-J07	NC	X*35, X*30	K02***C33-S01	NO
X*34	K07***D40-S01	NC	X*23, X*35	K00***D00-S01	NO
X*35	K01***D29-S01	NC	X*25, X*35	K02***E72-F01	NO

Note: Due to privacy concerns, the substation name is masked as * and ***.

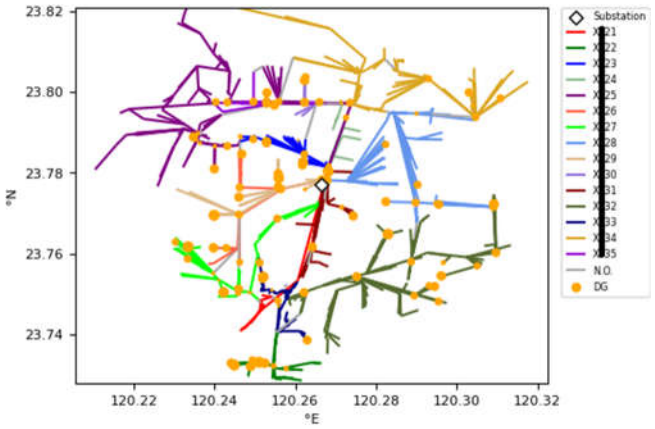

Figure 8. Geographic information of X* S/S (Due to privacy concerns, the substation name is masked by the black line).

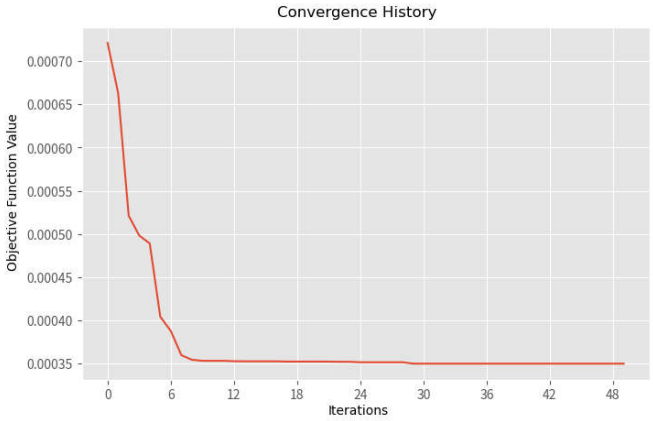

Figure 9. Convergence history of GWO.

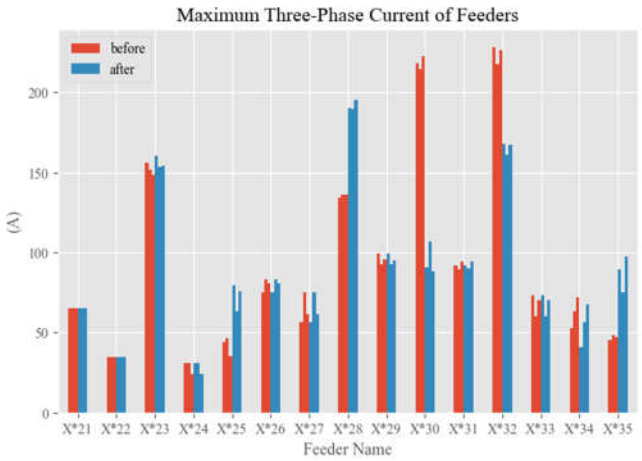

Figure 10. Maximum three-phase currents of each feeder in X* S/S.

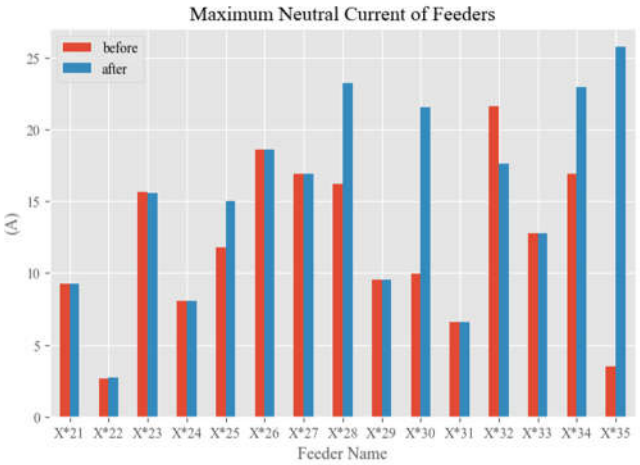

Figure 11. Maximum neutral currents of each feeder in X* S/S.

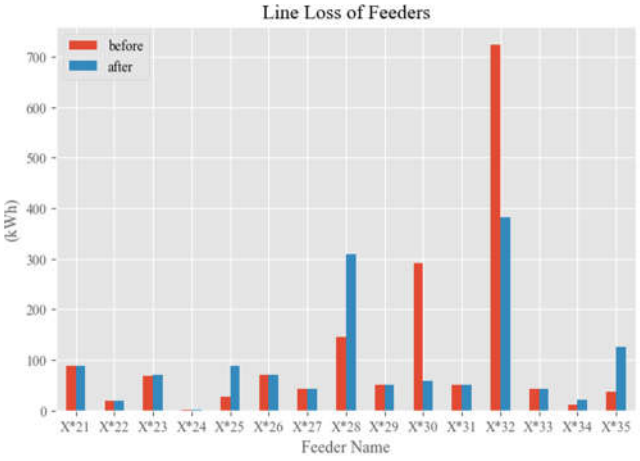

Figure 12. Total line losses of each feeder in X* S/S.

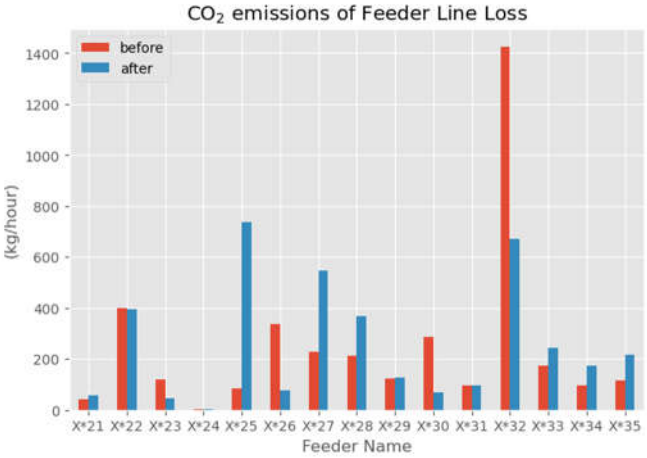

Figure 13. Total CO_2 emissions of each feeder in X* S/S.

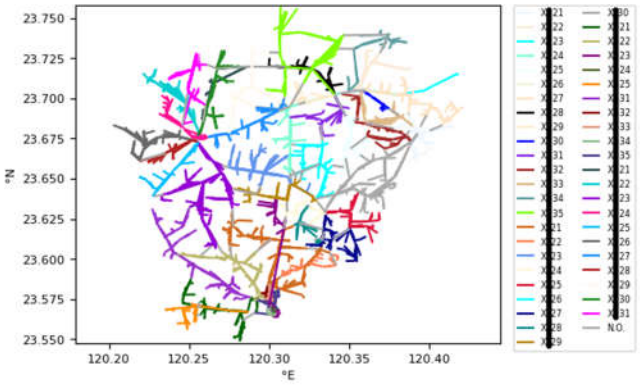

Figure 14. Geographic information of the 3 S/Ss.

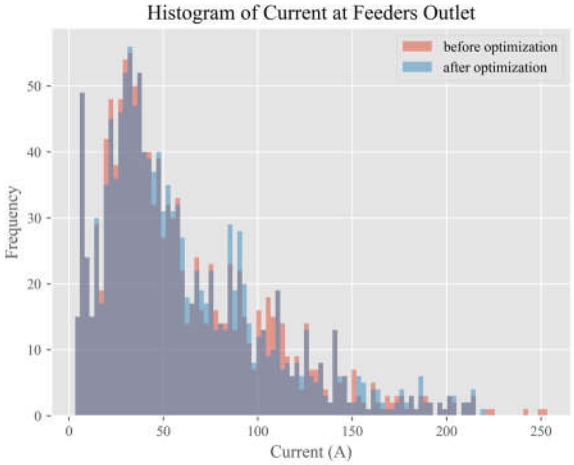

Figure 15. Histogram of the individual phase current at the feeder front in the 3 S/Ss (The orange color represents the result before optimization, and the blue color represents the result after optimization; furthermore, the purple-gray denotes the overlapping part of orange and blue).

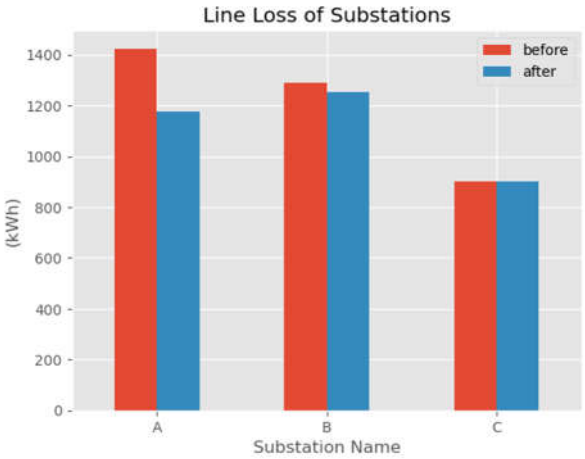

Figure 16. Total line losses of the 3 S/Ss.

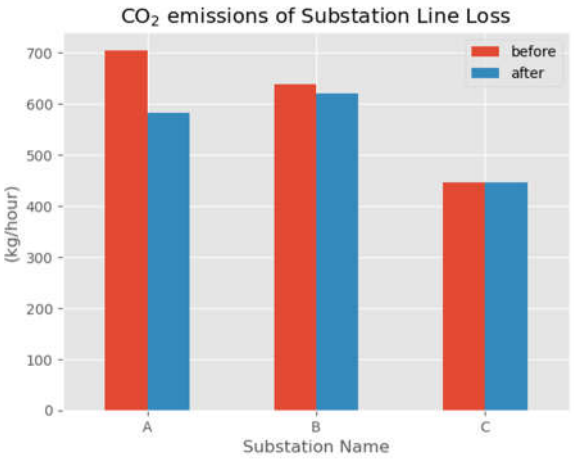

Figure 17. Total CO_2 emissions of the 3 S/Ss.

5. Conclusions

In this study, we developed a GADNRF aimed at reducing CO_2 emissions by uniformly distributing line currents and reducing line loss in ADNs through optimized switch operations during both the system planning and operational stages. The application focused on real ADNs within Taipower, with data sourced from the DMMS and SCADA systems of the DDCC. The approach for modeling ADNs was elucidated and implemented, including an NR algorithm designed to maintain radial topology within ADNs. This algorithm is universally applicable across ADNs without necessitating data preprocessing. A total of forty-two swarm algorithms were harnessed to explore optimal NR solutions. For user convenience, we designed a user-friendly interface tailored to ADN operators, enhancing the intuitive nature of the platform. In conclusion, we presented numerical simulation results for both single and multiple substations. These results demonstrated that the performance of the target ADNs, including factors such as total CO_2 emissions, line losses, and uniformly distributed feeder currents, surpassed that of the original system. The proposed platform holds considerable significance, offering an amalgamation of big data, swarm intelligence, and power flow analysis. The NR algorithm's suggested switch operations provided a systematic approach for distribution operators, offering a more objective methodology compared to relying solely on personnel experience. For future studies, this study can be extended to explore research topics related to NR. These may include enhancing the hosting capacity of modern distribution networks with a high penetration of DGs through NR, as well as implementing smart feeder load management to prevent feeder overloading and reverse power flow to the main transformers in distribution substations caused by DGs through NR.

Author Contributions: All authors contributed meaningfully to this study. Conceptualization, K.-C.Y.; data curation, C.-H.H.; methodology, W.-C.L.; resources, Y.-D.L.; software, Y.H.; supervision, W.-T.H.; visualization, J.-L.J. All authors have read and agreed to the published version of the manuscript.

Funding: This work was sponsored in part by the Institute of Nuclear Energy Research of Taiwan through its grant no. 111A009 and the National Science and Technology Council, Taiwan, under grant 112-2221-E-018-001-MY3.

Institutional Review Board Statement: Not applicable.

Informed Consent Statement: Not applicable.

Data Availability Statement: The data used in this research is enclosed within the manuscript. No external data sources are used in this research.

Conflicts of Interest: The authors declare no conflicts of interest.

References

1. Chen, T.H.; Huang, W.T.; Gu, J.C.; Pu, G.C.; Hsu, Y.F.; Guo, T.Y. Feasibility study of upgrading primary feeders from radial and open-loop to normally closed-loop arrangement. *IEEE Trans. Power Syst.* **2004**, *19*, 1308–1316.
2. Yan, X.; Zhang, Q. Research on Combination of Distributed Generation Placement and Dynamic Distribution Network Reconfiguration Based on MIBWOA. *Sustainability* **2023**, *15*, 9580. https://doi.org/10.3390/su15129580.
3. Alanazi, A.; Alanazi, T.I. Multi-Objective Framework for Optimal Placement of Distributed Generations and Switches in Reconfigurable Distribution Networks: An Improved Particle Swarm Optimization Approach. *Sustainability* **2023**, *15*, 9034. https://doi.org/10.3390/su15119034.
4. Kandasamy, M.; Thangavel, R.; Arumugam, T.; Jayaram, J.; Kim, W.-W.; Geem, Z.W. Performance Enhancement of Radial Power Distribution Networks Using Network Reconfiguration and Optimal Planning of Solar Photovoltaic-Based Distributed Generation and Shunt Capacitors. *Sustainability* **2022**, *14*, 11480. https://doi.org/10.3390/su141811480.
5. Gallego Pareja, L.A.; López-Lezama, J.M.; Gómez Carmona, O. Optimal Feeder Reconfiguration and Placement of Voltage Regulators in Electrical Distribution Networks Using a Linear Mathematical Model. *Sustainability* **2023**, *15*, 854. https://doi.org/10.3390/su15010854.
6. Yin, Z.; Ji, X.; Zhang, Y.; Liu, Q.; Bai, X. Data-driven approach for real-time distribution network reconfiguration. *IET Gener. Transm. Distrib*. **2020**, *14*, 2450–2463.
7. Gangwar, P.; Singh, S.N.; Chakrabarti, S. Network reconfiguration for the DG-integrated unbalanced distribution system. *IET Gener. Transm. Distrib*. **2019**, *13*, 3896–3909.
8. Tuladhar, S.R.; Singh, J.G.; Ongsakul, W. Multi-objective approach for distribution network reconfiguration with optimal DG power factor using NSPSO. *IET Gener. Transm. Distrib.* **2016**, *10*, 2842–2851.
9. Noebels, M.; Preece, R.; Panteli, M. A machine learning approach for real-time selection of preventive actions improving power network resilience. *IET Gener. Transm. Distrib.* **2022**, *16*, 181–192.
10. Huang, W.; Zheng, W.; Hill, D.J. Distribution Network Reconfiguration for Short-Term Voltage Stability Enhancement: An Efficient Deep Learning Approach. *IEEE Trans. Smart Grid* **2021**, *12*, 5385–5395.
11. Gholizadeh, N.; Kazemi, N.; Musilek, P. A Comparative Study of Reinforcement Learning Algorithms for Distribution Network Reconfiguration with Deep Q-Learning-Based Action Sampling. *IEEE Access* **2023**, *11*, 13714–13723.
12. Wang, B.; Zhu, H.; Xu, H.; Bao, Y.; Di, H. Distribution Network Reconfiguration Based on NoisyNet Deep Q-Learning Network. *IEEE Access* **2021**, *9*, 90358–90365.
13. Takenobu, Y.; Yasuda, N.; Kawano, S.; Minato, S.I.; Hayashi, Y. Evaluation of Annual Energy Loss Reduction Based on Reconfiguration Scheduling. *IEEE Trans. Smart Grid* **2018**, *9*, 1986–1996.
14. Gangwar, P.; Mallick, A.; Chakrabarti, S.; Singh, S.N. Short-Term Forecasting-Based Network Reconfiguration for Unbalanced Distribution Systems with Distributed Generators. *IEEE Trans. Ind. Inform.* **2020**, *16*, 4378–4389.
15. Wu, Y.; Liu, J.; Wang, L.; An, Y.; Zhang, X. Distribution Network Reconfiguration Using Chaotic Particle Swarm Chicken Swarm Fusion Optimization Algorithm. *Energies* **2023**, *16*, 7185. https://doi.org/10.3390/en16207185.
16. Botea, A.; Rintanen, J.; Banerjee, D. Optimal Reconfiguration for Supply Restoration with Informed Search. *IEEE Trans. Smart Grid* **2012**, *3*, 583–593.
17. Peng, C.; Xu, L.; Gong, X.; Sun, H.; Pan, L. Molecular Evolution Based Dynamic Reconfiguration of Distribution Networks with DGs Considering Three-Phase Balance and Switching Times. *IEEE Trans. Ind. Inform.* **2019**, *15*, 1866–1876.
18. Swaminathan, D.; Rajagopalan, A.; Montoya, O.D.; Arul, S.; Grisales-Noreña, L.F. Distribution Network Reconfiguration Based on Hybrid Golden Flower Algorithm for Smart Cities Evolution. *Energies* **2023**, *16*, 2454. https://doi.org/10.3390/en16052454.
19. Shaheen, A.; El-Sehiemy, R.; Kamel, S.; Selim, A. Optimal Operational Reliability and Reconfiguration of Electrical Distribution Network Based on Jellyfish Search Algorithm. *Energies* **2022**, *15*, 6994. https://doi.org/10.3390/en15196994.
20. Chen, Q.; Wang, W.; Wang, H.; Wu, J.; Li, X.; Lan, J. A Social Beetle Swarm Algorithm Based on Grey Target Decision-Making for a Multiobjective Distribution Network Reconfiguration Considering Partition of Time Intervals. *IEEE Access* **2020**, *8*, 204987–205013.
21. Lakra, N.S.; Bag, B. Loss Minimization of Distribution System via Network Reconfiguration using Meta-heuristic Algorithm. In Proceedings of the 2021 7th International Conference on Electrical Energy Systems (ICEES), Online, 11–13 February 2021; pp. 225–228.
22. Gerez, C.; Silva, L.I.; Belati, E.A.; Sguarezi Filho, A.J.; Costa, E.C. Distribution network reconfiguration using selective firefly algorithm and a load flow analysis criterion for reducing the search space. *IEEE Access* **2019**, *7*, 67874–67888.
23. Muhammad, M.A.; Mokhlis, H.; Naidu, K.; Amin, A.; Franco, J.F.; Othman, M. Distribution Network Planning Enhancement via Network Reconfiguration and DG Integration Using Dataset Approach and Water Cycle Algorithm. *J. Mod. Power Syst. Clean Energy* **2020**, *8*, 86–93.
24. Esmaeilian, H.R.; Fadaeinedjad, R. Energy Loss Minimization in Distribution Systems Utilizing an Enhanced Reconfiguration Method Integrating Distributed Generation. *IEEE Syst. J.* **2015**, *9*, 1430–1439.
25. Srinivasa, R.; Rao, S.V.L.; Narasimham, M.; Raju, M.R.; Rao, A.S. Optimal Network Reconfiguration of Large-Scale Distribution System Using Harmony Search Algorithm. *IEEE Trans. Power Syst.* **2011**, *26*, 1080–1088.
26. Fu, Y.; Chiang, H. Toward Optimal Multiperiod Network Reconfiguration for Increasing the Hosting Capacity of Distribution Networks. *IEEE Trans. Power Deliv.* **2018**, *33*, 2294–2304.

27. Gong, H.; Jones, E.S.; Jakaria, A.H.; Huque, A.; Renjit, A.; Ionel, D.M. Large-Scale Modeling and DR Control of Electric Water Heaters with Energy Star and CTA-2045 Control Types in Distribution Power Systems. *IEEE Trans. Ind. Appl.* **2022**, *58*, 5136–5147.
28. *IEC 61850*; Communication Networks and Systems for Power Utility Automation. International Electrotechnical Commission: Geneva, Switzerland, 2013.
29. Prasad, K.; Ranjan, R.; Sahoo, N.C.; Chaturvedi, A. Optimal reconfiguration of radial distribution systems using a fuzzy mutated genetic algorithm. *IEEE Trans. Power Deliv.* **2005**, *20*, 1211–1213.
30. Sekhavatmanesh, H.; Cherkaoui, R. A Multi-Step Reconfiguration Model for Active Distribution Network Restoration Integrating DG Start-Up Sequences. *IEEE Trans. Sustain. Energy* **2020**, *11*, 2879–2888.
31. Tang, J.; Liu, G.; Pan, Q. A Review on Representative Swarm Intelligence Algorithms for Solving Optimization Problems: Applications and Trends. *IEEE/CAA J. Autom. Sin.* **2021**, *10*, 1627–1643. https://doi.org/10.1109/JAS.2021.1004129.